Widespread forest cutting in the aftermath of World War II captured by broad-scale historical Corona spy satellite photography

Article *in* Remote Sensing of Environment · October 2017

DOI: 10.1016/j.rse.2017.10.021

CITATION
1

READS
405

5 authors, including:

Mihai Daniel Nita
Universitatea Transilvania Brasov
31 PUBLICATIONS **69** CITATIONS
SEE PROFILE

Catalina Munteanu
Leibniz Institute of Agricultural Development in Transition Economies (IAMO) and …
20 PUBLICATIONS **414** CITATIONS
SEE PROFILE

Garik Gutman
NASA
92 PUBLICATIONS **3,788** CITATIONS
SEE PROFILE

Ioan Vasile Abrudan
Universitatea Transilvania Brasov
73 PUBLICATIONS **869** CITATIONS
SEE PROFILE

Remote Sensing of Environment 204 (2018) 322–332

Contents lists available at ScienceDirect

Remote Sensing of Environment

journal homepage: www.elsevier.com/locate/rse

Widespread forest cutting in the aftermath of World War II captured by broad-scale historical Corona spy satellite photography

Mihai Daniel Nita[a,b,*], Catalina Munteanu[b,c,d], Garik Gutman[e], Ioan Vasile Abrudan[a], Volker C. Radeloff[b]

[a] Department of Forest Engineering, Faculty of Silviculture and Forest Engineering, Transilvania University of Brasov, 1 Sirul Beethoven, Brasov, Romania
[b] SILVIS Lab, Department of Forest and Wildlife Ecology, University of Wisconsin-Madison, 1630 Linden Drive, Madison, WI 53706, USA
[c] Leibniz Institute of Agricultural Development in Transition Economies (IAMO), Theodor Lieser Straße 2, 06120 Halle (Saale), Germany
[d] Geography Department, Humboldt University Berlin, Unter den Linden 6, 10099 Berlin, Germany
[e] NASA Land Use and Land Cover Change Program, Washington, DC 20546, USA

ARTICLE INFO

Keywords:
Declassified satellite photography
Structure from Motion
Historical deforestation
Disturbance mapping
Corona spy satellite

ABSTRACT

Wars have major economic, political and human implications, and they can strongly affect environment and land use, not only during the conflicts, but also afterwards. However, data on the land use effects of wars is sparse, especially for World War II, the largest war in history. Our goal was to quantify and understand the time-lagged land use effects of WWII in Romania, by applying Structure from Motion technology to 1960s Corona spy satellite photography. We quantified forest cutting across Romania from 1955 to 1965. This was a period when Romania's economy recovered from the war and when Romania established close economic ties to the Soviet Union, and when the Romanian government made reparation payments to the Soviet Union. To understand the effects of war, we developed an accurate and fast method to orthorectify high-resolution Corona photography in mountain areas, and rectified scanned Corona photography based on Structure from Motion technology. Our study area of 212,000 km^2 was covered by 208 Corona film strips, which we rectified with an overall average accuracy of 14.3 m. We identified 530,000 ha of forest cuts over this time period, the rate of which is three times higher than contemporary cutting rates. Our results highlight that the environmental and land use effects of WWII were substantial in Romania, due to reparation payments, post-war policies regarding resource exploitation, and technological and infrastructural development. Our research provides quantitative evidence of how wars can cause time-lagged and long-term effects on the environment. Methodologically, we advance remote sensing science by pioneering a new approach to orthorectify Corona photography for large areas effectively. Corona data are available globally. Our approach facilitates the extension of the data record of space borne observation of the earth by one to two decades earlier than what is possible with satellite datasets.

1. Introduction

Land use change is a major aspect of global change (Foley et al., 2005; Vorovencii, 2014) but rates of land use change are typically gradual (Dinca et al., 2017; Geist and Lambin, 2004; Kozak et al., 2007; Müller et al., 2013). However, when shocks - such as wars - occur, land use and land cover changes can be rapid and unpredictable (Baumann and Kuemmerle, 2016; Bouma et al., 1998; Lambin et al., 2003). The immediate effects of wars on the environment can be substantial (Baumann et al., 2014; Rudel et al., 2005), but there are likely also time-lagged and long-term land use effects of wars, which remain largely unknown (Robinson and Sutherland, 2002). Time-lagged effects of wars can be due to, for example, reparation payments following conflict, or rebounding economies following a war, a phenomenon known as the Phoenix factor (Humphreys, 2005; Organski and Kugler, 1977), which occurs typically about 15–20 years after major conflicts (Kim et al., 2014; Organski and Kugler, 1977). However, a given country's economical and socio-political development may affect this timing, where the least developed societies are likely to deteriorate for long periods after wars (Fisunoglu, 2014; Hasic, 2004), whereas more developed countries rebound faster. Given this, it is important to increase the understanding of the time-lagged effects of wars on land use and the environment (Baumann et al., 2014; Burgess et al., 2015).

The largest war in history was the Second World War (WWII, 1939–1945), which had major economic, political and human implications, both during the conflict, and afterwards. The economic and

* Corresponding author at: Department of Forest Engineering, Faculty of Silviculture and Forest Engineering, Transilvania University of Brasov, 1 Sirul Beethoven, Brasov, Romania.
E-mail address: mihai.nita@unitbv.ro (M.D. Nita).

http://dx.doi.org/10.1016/j.rse.2017.10.021
Received 19 April 2017; Received in revised form 5 October 2017; Accepted 13 October 2017
Available online 24 October 2017
0034-4257/

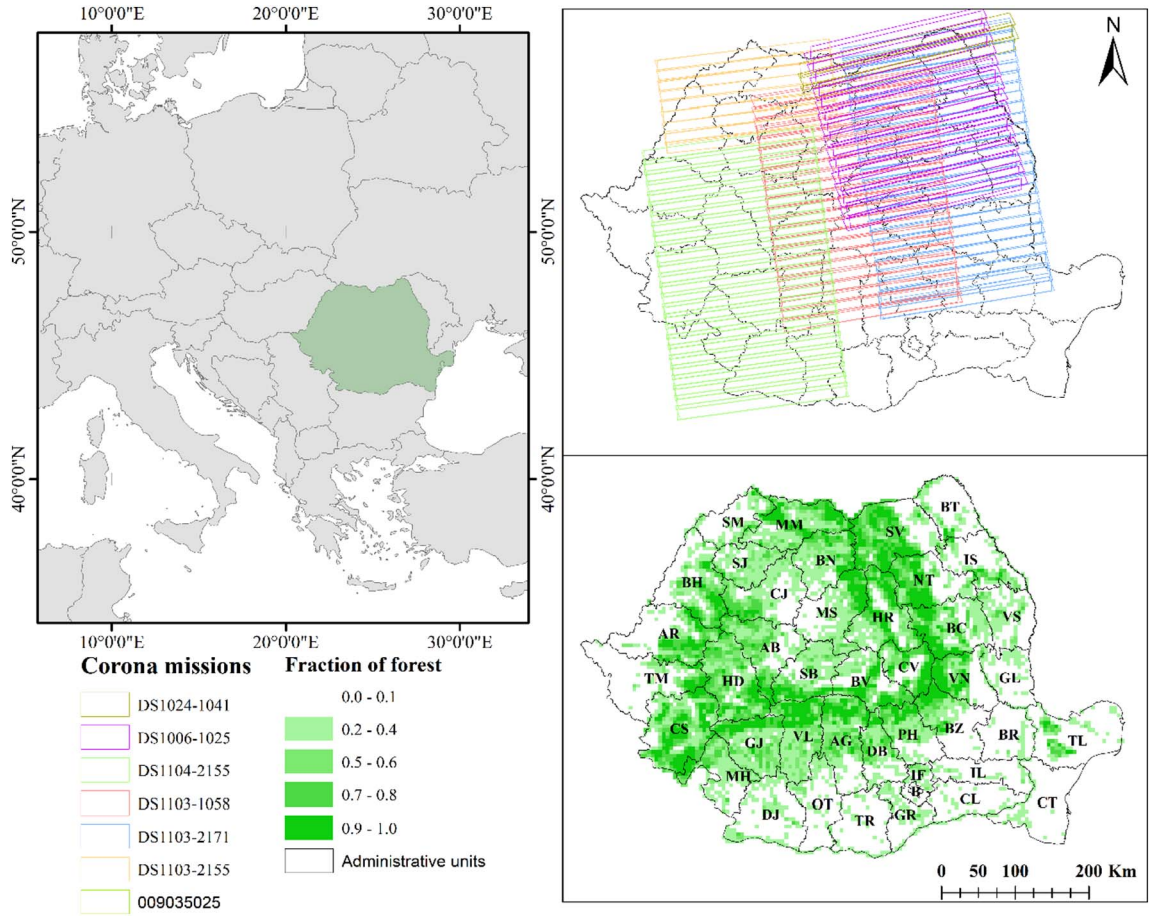

Fig. 1. Location of Romania within Europe (left), coverage of the 208 Corona spy satellite photographs (104 stereo pairs) of seven different mission (top right), and percent forest cover in 1970 (5-km resolution, bottom right).

fiscal collapse of many countries immediately following the war (Bakacsi et al., 2002; Brenner, 2003; Eichengreen, 1945) was due to the loss of human capital, lack of education for young children, and reduced earnings (Ichino and Winter-Ebmer, 2004). Military actions during WWII also caused widespread environmental effects, including soil compaction and vegetation changes (Machlis and Hanson, 2011), contamination of marine life (Martins et al., 2006) and introduction of invasive species (Fritts and Rodda, 1998; Kim, 1997).

In the post-war period (1947–1956), the Soviet Union government secured large reparation payments from East Germany and much of Eastern Europe, which likely even exceeded the $10 billion dollars that it had negotiated at Yalta (DeConde, 1978; Herman, 1951; Parrini and Matray, 2002). Many of the reparation payments were made in form of natural resources, such as timber, which may have had long-lasting environmental and land use effects beyond the immediate harvests. The resulting infrastructural developments facilitated further resource use even after reparations have been fully paid, and historical land use likely caused land use legacies that persist (Munteanu et al., 2016; Munteanu et al., 2015). Furthermore, as the main actor of the economic development of Eastern Europe, the Soviet Union implemented the Stalinist strategy of industrialization and central planning, especially in the “allied” countries (Czechoslovakia, Poland, Yugoslavia), and they established either fully Soviet-owned companies (Hungary, Bulgaria), or joint companies (Romania) that delivered their profits to the Soviet Union (Banu, 2004; Bekes et al., 2015; Ben-ner and Montias, 2015; Gibianskii and Naimark, 2006; Tamas, 1987).

Unfortunately, there are limited data on the environmental effects of WWII, partly because remote sensing data for broad scale analysis only became available with the launch of the first Landsat satellites in 1972 (Roy et al., 2014). The US government did collect space borne photography globally for strategic intelligence decades prior to the first Landsat satellite, and these data remained classified until 1996 (Galiatsatos et al., 2004; McDonald, 1995). Corona images provide space borne photography for the decades immediately following the WWII (Song et al., 2014) and are well suited for land use mapping (Beck et al., 2007; Challis et al., 2002; Day, 2015). Prior studies using Corona images have monitored boreal forest decline (Rigina, 2003), vegetation dynamics (Kadmon and Harari-Kremer, 1999), land use change (Tappan et al., 2000), carbon emissions from forest fires (Isaev et al., 2002), ice sheet change (Bindschadler and Vornberger, 1998; Grosse et al., 2005), and archaeological features (Beck et al., 2007; Casana and Cothren, 2008; Challis et al., 2002). However, because ortho-rectifying Corona images is complex and time-consuming (Sohn et al., 2004; Song et al., 2014; Tappan et al., 2000), and due to the lack of information about a given mission's sensor (Hamandawana et al., 2007; Peebles, 1997; Sohn et al., 2004; Zhou et al., 2003), high level of spatial distortion (Casana and Cothren, 2008; Sohn et al., 2004; Song et al., 2014), and scanning errors (Gheyle et al., 2011), there have been relatively few land use studies using Corona photographs, and they have typically been limited in their spatial extent.

A potential alternative approach to ortho-georectifying Corona Images is to use structure from Motion (SfM) algorithms (Ullman, 1979). SfM has been used for land monitoring, especially when there is a need for three-dimensional data, because it is cheaper to acquire point clouds from optical data with SfM than from LIDAR data (Burns et al., 2010; Clinciu and Nita, 2011; Delparte et al., 2014; Harwin and Lucieer, 2012). SfM is also advantageous when the intrinsic camera parameters are varying or unknown, as is the often case when analyzing

imagery from drones or close-range terrestrial photogrammetry (Burns et al., 2015; Caroti et al., 2015; Fonstad et al., 2013; Ouédraogo et al., 2014; Pollefeys et al., 1999). However, SfM has rarely been applied to historical photography for large areas (Casana and Cothren, 2013; Gomez, 2012; Verhoeven et al., 2012), and to the best of our knowledge never to Corona imagery, although it may be well suited for this task.

Our overarching goal was to quantify and understand the time-lagged environmental and land use effects of WWII in Romania by applying Structure from Motion technology to an underused remote sensing resource from the 1960s, the Corona photographs. Our specific goals were to 1) develop an accurate and fast method to orthorectify Corona images in mountainous areas, 2) quantify the amount of forest harvest in Romania from 1955 to 1965, and 3) analyze the spatial distribution and patterns of harvested patches.

2. Methods

2.1. Study area

We studied forest harvest following WWII in Romania (238,381 km^2), which is heavily forested, especially in and around the Carpathian Mountains (European Environment Agency, 2003). Romania's climate is temperate, (Fig. 1), and mean elevation is 330 m (0–2544 m, (Spârchez et al., 2013)). About 18% of our study region has rugged terrain (> 15° slope), the rest is relatively flat (< 5°, 52%), or rolling (5–15°, 30%) (USGS, 2004).

Romania experienced severe shocks due to WWII, both economically and environmentally. After WWII, the country had to make reparation payments to the Soviet Union in the form of natural resources such as petroleum, mineral and timber (Bancila, 2016; Bekes et al., 2015; Ben-ner and Montias, 2015; Giurescu, 1976). Furthermore, until 1958, the Soviet Union imposed polices that put pressure on natural resources (Bekes et al., 2015). Under joint Soviet-Romanian economic ventures (SOVROM), Romania was to provide 1 million cubic meters of timber annually to the Soviet Union (Banu, 2004; Bekes et al., 2015), plus other natural resources (e.g. petroleum, natural gas, and uranium), in exchange for knowledge and infrastructure development (Bancila, 2016; Ben-ner and Montias, 2015; Constantinescu, 1953).

Romania had extensive forest resources at the end of WWII. In 1946, approximately 26% of the country was forested, with a high proportion of coniferous forests in the mountains (*Picea abies*-spruce and *Abies alba*-fir) as well as ecologically valuable deciduous forests (e.g., *Quercus sp.*-oak) (Munteanu et al., 2016). Furthermore, based on Soviet reports, Romania had approximately 1 million ha of so-far inaccessible old-growth forests that might become available for harvesting with additional road construction (Banu, 2004; Ivanescu, 1972). As a result, anecdotal evidence suggests that much of the country's mature forest cover was harvested in the aftermath of WWII (Marea Adunare Nationala, 1976), but a detailed assessment of post-war harvesting has been lacking.

2.2. Data

We obtained declassified photographic data acquired by seven Corona missions (Song et al., 2014) from 1962 to 1968 from the U.S. Geological Survey (Fig. 1). Specifically, we analyzed 208 scanned, panchromatic, medium and high stereographic coverage Corona images, grouped in 104 stereo pairs (Table 1). Each scanned film strip covers approximately 17 × 230 km on the ground (Sohn et al., 2004).

These 208 images provide a nearly-full coverage of Romania's forests with 1.83–2.74 m resolution (Fig. 2). For areas that were out-of-focus or partially cloud covered, we used more than one image pair.

2.3. Overview of the rectification methodology using Structure from Motion (SfM) technology

For the geo-rectification of the stereo-pairs we employed Structure from Motion (SfM) bundle adjustment as implemented in AgiSoft Photoscan (Fig. 3). We divided the process into four steps: 1) aligning photos, 2) point cloud georeferencing, 3) digital surface model extraction, and 4) orthophoto generation (Agisoft LLC, 2011).

In the first step, we used a procedure based on detecting and matching image features to align the photos. The algorithm estimates camera parameters such as focal length in x,y dimensions, principal point coordinates, skew transformation coefficient, and radial and tangential distortion coefficients, using only the relation between the images (Agisoft LLC, 2011; Heikkila and Silven, 1997; Lucchese, 2005; Slama et al., 1980). SfM matches individual pixels between the images independent of geometric transformations and instead based on information from neighboring pixels (Apollonio et al., 2014; Harris, 1993; Lowe, 2004). The algorithm detects points in both source photos that are stable under different viewpoint and lighting conditions, depending on the camera position (Agisoft LLC, 2011; Ouédraogo et al., 2014) and identifies tie points (TP) between images. Because data about flight, camera, image and film parameters were either unavailable or incomplete for Corona photographs (Dashora et al., 2007; Galiatsatos et al., 2004; Kim et al., 2007), we utilized the Agisoft Photoscan algorithm, and the derived tie points to estimate the intrinsic camera parameters. Based on the tie points and the intrinsic camera parameters, we computed the 3D points in a synthetic coordinate system that was not connected to a real-world coordinate system (Agisoft LLC, 2011).

In the second step we assigned real-world coordinates to the point-cloud, by calculating the extrinsic orientation parameters of the camera using the relation between the point cloud coordinates and ground control points (GCPs). To calculate this relation, we used the Helmert 3D transformation (Watson, 2006). We selected GCPs for each stereographic pair and distributed 20–30 points per pair evenly across the area and at different altitudes (Fig. 3). The ground x,y and z coordinates for GCPs were derived from an aerial image mosaic from 2010 provided as WMS (Web Map Service) from National Cadaster Agency, and from the Shuttle Radar Topographic Mission (SRTM) data for elevation (ANCPI, 2010; USGS, 2004). We aimed for an average locational error of 15 m for the entire scene. If the error was higher, we added more GCPs and recalculated the extrinsic orientation parameter (Fig. 3).

In the third step, we extracted the digital surface model, which is important for the orthorectification of the Corona images. The precision and resolution of the digital surface model greatly affects the accuracy of the final product, especially in mountainous areas (Altmaier and Kany, 2002; Popescu et al., 2003; Verhoeven et al., 2012). To extract a precise digital surface model from the point cloud, we used the exact smooth method, which is based on pair-wise depth map computation (Agisoft LLC, 2011). To extract a high resolution digital surface model, we calculated the depth information for each camera and combined it into a single dense point-cloud. We built the digital surface model by interpolating the dense points with an Inverse Distance Weighting interpolation (Agisoft LLC, 2011; Henley, 2012).

In the fourth and final step, we generated the orthophotos based on the relation between original Corona images and the digital surface model and compiled a full area coverage orthophoto mosaic. (Agisoft LLC, 2011; Lerma et al., 2006).

2.4. Georectification accuracy assessment

We quantified the processing time for each stereographic pair that we analyzed, and tested the positional accuracy after georectification for the horizontal axes x and y, and the total 3D error, using the previously selected Ground Control Points (GCP). To assess what affected georectification accuracy, we summarized the total error by camera

Table 1
Corona mission data and observations.

Mission ID	Launch date	Number of images	Camera type	Comments[a]
009035025	30 May 1962	4	Stereo medium	Slight Corona static on film
1006–1025	04 Jun 1964	30	Stereo medium	Highest-quality imagery attained to date from the KH-4 system
1024–1041	22 Sep 1965	4	Stereo medium	All cameras operated satisfactorily
1103–2155	01 May 1968	18	Stereo high	
1103–2171	01 May 1968	54	Stereo high	Out-of-focus imagery is present on both main camera records
1103–1058	01 May 1968	46	Stereo high	Out-of-focus imagery is present on both main camera records
1104–2155	07 Aug 1968	52	Stereo high	Best imagery to date on any KH-4 systems
	Total	208		

[a] (National Reconnaissance Office, 2005).

type, image quality, major morphological classes, and slope. For continuous variables, we calculated their correlation with the overall error. For categorical variables, we ran two-sample *t*-tests, and Tukey multiple comparisons of means to test if certain categories had higher overall error. Additionally we created an independent and random validation point dataset containing 400 random points distributed across the different Corona missions.

2.5. Forest disturbance mapping

For the forest harvest analysis, we mosaicked the 104 orthophotos and digitized all forest disturbances using standard visual interpretation techniques. We defined forest disturbance as loss of forest cover, including clear-cuts, final-cuts in shelterwood systems, windthrows, and insect attacks that were visually apparent in the pan-chromatic image mosaics due to differences in image texture, gray level and patch size (Fig. 4). To differentiate the disturbances from pastures or other visually similar areas we used a forest cover mask extracted from the 1970 topographic map of Romania (Directia Topografica Militara, 1975). Based on our estimate, visible disturbances in the Corona mosaic stemmed from forest disturbances from 1955 to 1965. We chose this 10 year period based on forest regeneration rates observed in other remote sensing studies in the Carpathians (Hansen et al., 2013; Potapov et al., 2015). Additionally, we tested the rate of forest regeneration in terms of how texture and grayscales changed over time, by examining Corona images from successive years (i.e., 1962, 1964, 1968) for selected areas.

For our accuracy assessment, we validated 10% of the disturbance mapping areas based on average stand age as reported in decadal forest management maps provided by the National Forestry Administration via a memorandum of understanding with Transilvania University of Brasov. The Romanian forest management maps contain information at the stand level about tree composition, stand age, canopy cover, and production class (Doniţă, 2014). We estimated the harvest year based on the stand age plus the year the stand was inventoried. We compared our digitized disturbance data with the approximate harvest year derived from the forest management maps, and checked if the year was within 1955–1965.

To quantify the patterns of forest disturbance across Romania, we summarized the percentage of harvested forest for a 5-km grid. In addition, we assessed the number of harvested patches, as well as the harvested areas, and the patch size by major geomorphologic units and forest types (Donita et al., 1960; geo-spatial.org, 2008). To assess if there are long-term effects on contemporary forest changes, we compared the historic harvests with current forest composition data, i.e., the extent of spruce monocultures.

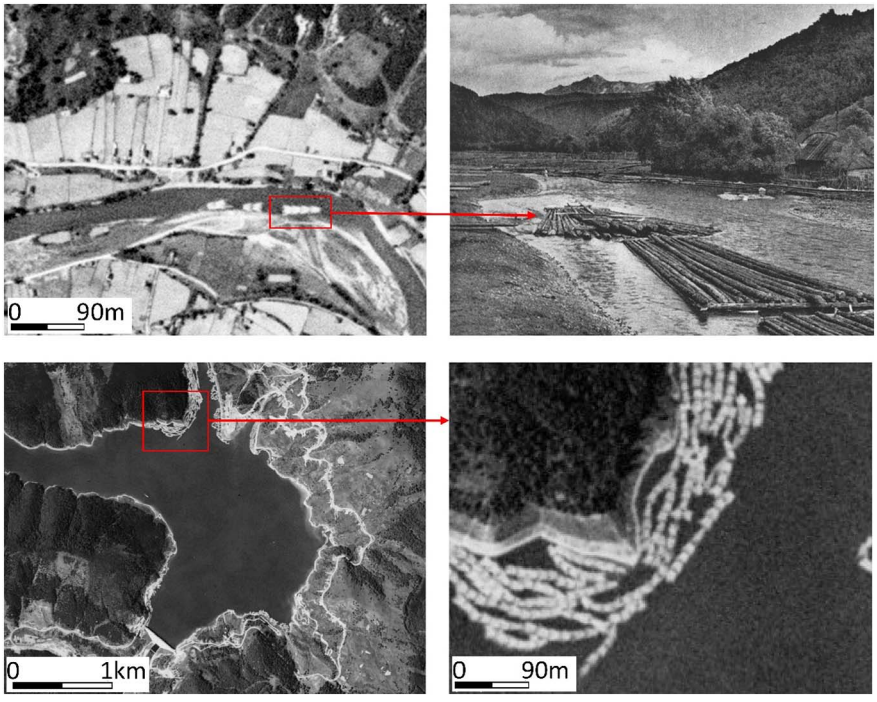

Fig. 2. Example of Corona photographs showing timber rafts on the Bistrita River (top left) and on Izvorul Muntelui Lake (bottom right and left) in DS1006-1025DA077 Corona Image (2-m resolution) from June 4th 1964. Historic photography of timber rafts from the same period show the typical shape of the rafts (top right, image source: http://www.carpati.org).

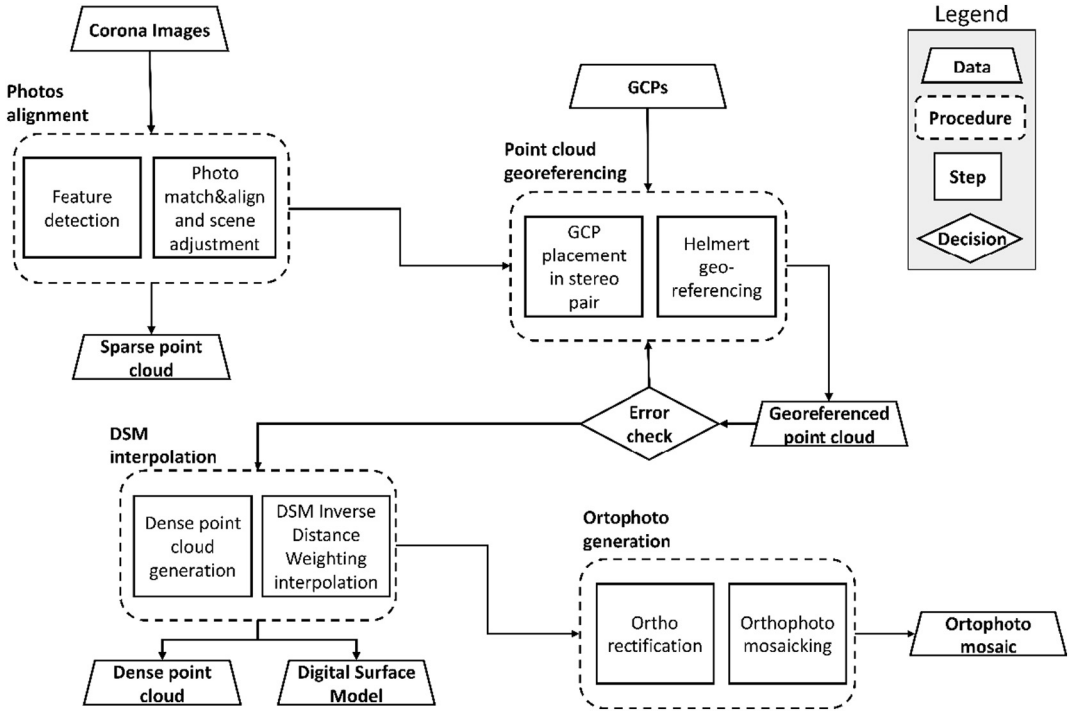

Fig. 3. Corona image ortho-geo-rectification workflow using Structure from Motion algorithms, including four major work steps: photo alignment, point cloud referencing, digital surface model interpolation and orthophoto generation.

3. Results

We successfully rectified 208 Corona pairs with an average accuracy of ≤ 15 m, and mapped 530,000 ha of forest cutting in Romania from 1955 to 1965, which highlights the magnitude of the long-term land use effects of WWII on Romania's forests.

3.1. Method robustness and georectification accuracy assessment

Our accuracy assessment showed an average absolute horizontal error of 14.3 m for the entire study region, with errors ranging from as little as 0.3 m in flat areas and for images with good image quality, to as much as 43.4 m in rugged terrain and for images with low quality. Almost 59% of our points had errors < 15 m, 37% were between 15 and 30 m, and only 5% of the points had errors > 30 m (Table 2). In terms of vertical accuracy, the average error was 2.24 m (−60.6 to 53.2 m), 40% of the points had errors < 15 m, 30% between 15 and 30 m, and 30% > 30 m (Fig. 5).

When we analyzed the total error in relation to geomorphological conditions and image attributes, we found that points in mountainous regions had substantially higher errors (20.2 m) that those in flat terrain (3.6 m, $p < 0.001$). Image quality also substantially influenced errors. Low-quality images had significantly higher error (15.5 m) than high quality images (mean error 13.6 m, $p < 0.001$), but there was no significant difference between low- and medium-quality images. Furthermore, we found no significant effects of camera type ($p = 0.780$), elevation ($p = 0.848$), slope direction ($p = 0.602$) and geographic coordinates on errors (Table 2).

When we analyzed the accuracy of the model, based on random validation point dataset, the accuracy assessment showed an average absolute horizontal error of 14.01 m for the entire study region. We found no significant difference between the results for the random points and those for the previously collected GCPs, which is why we did not repeat the analysis of the causes of the errors for the random points.

On average, it took 152 min to orthorectify a Corona stereographic pair on a Windows-based Server with 48 cores and 512 Gb of RAM. The average time for photo alignment and scene estimation was 8 min/photo pair; the most time-consuming step in the process was the point cloud geo-referencing which took about 125 min/photo pair. Using a single experienced operator, it took an average of 5 min/photo pair to identify and assign 1 ground control point, and an average of 25 points for meeting the desired accuracy. The orthophoto generation based on the digital surface model extraction took on average 21 min/photo pair.

3.2. Forest disturbance mapping

We found that out of the total 6,100,000 ha of forest cover in 1950 (Munteanu et al., 2016), 530,000 ha were harvested from 1955 to 1965. We mapped 10,505 harvest patches, most of them in spruce, beech and mixed beech-spruce forests. The forest harvests covered 8.7% of the total forest area. Most of the disturbances were concentrated in the northern part of the eastern Romanian Carpathians (Fig. 6), but large harvests also occurred in the western southern Carpathians, and in the central part of the western Romanian Carpathians. The average size of harvested patches was 50.5 ha, but at elevations higher than 500 m, the average patch size was 123 ha, and individual cuts were as large as 11,700 ha (Table3).

We found that the largest harvests were concentrated in mountain areas and affected mostly mixed beech and spruce forests, with smaller (average 43 ha) and clustered patches in hilly areas. Most the harvests occurred on steep slopes (> 10°). Spruce, mixed beech-spruce and beech forests were generally targeted for harvest, with a total of 35% of the harvest (190,000 ha) occurring in beech forests, and another 35% in mixed beech and spruce forests (Table 3).

When we cross-checked our disturbance data versus contemporary forest age according to the forest management plans of selected areas, we found that for 98% of the areas, the age distribution data coincided with disturbances mapped from Corona (Fig. 7). The average forest management year for cross-checking the disturbance data was 1959.5.

Last but not least, when we investigated the potential long term effects of historic harvests by cross-tabulating harvests in the 1960s with contemporary forest composition based on Corine Land Cover 2012 and pre-harvest forest composition (Munteanu et al., 2016), we found that of all the 1960s harvests, 32% were contemporary spruce monocultures (Supplementary Material).

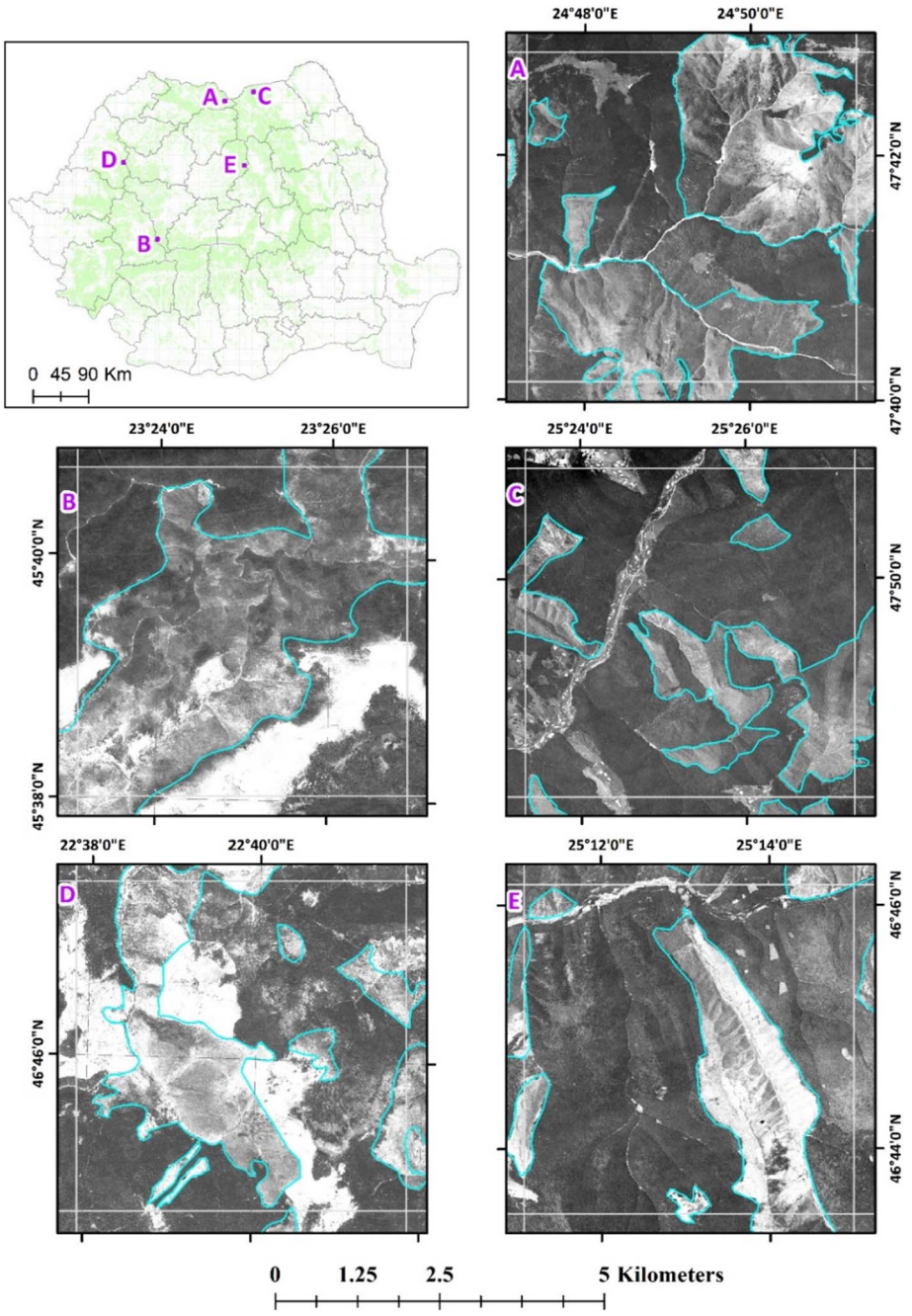

Fig. 4. Forest cover in Romania in year 1970 (top left), and five 5 × 5 km cell examples of forest disturbance in Corona photographs. A: Maramures (1964), B: Hunedoara (1968), C: Suceava (1964), D: Bihor (1968), E: Mures (1964). Blue lines represent the digitized disturbed areas and gray lines represent the cell limit. (For interpretation of the references to color in this figure legend, the reader is referred to the web version of this article.)

4. Discussion

We present here a substantial methodological advancement by developing an accurate, robust and fast method to orthorectify Corona photographs, which allowed us to extend the time horizon of space borne earth observation by over a decade prior to the first Landsat images. By applying this methodology, we were able to map post-WWII forest harvests across Romania for a total area of 212,000 km^2. We identified widespread forest cutting, with rates that were three times higher than the contemporary harvest rates. Our results suggest that time-lagged environmental effects of WWII were substantial in Romania. We attribute these effects to post-war socio-economic and political decisions such as reparation payments and related infrastructural development. Our results suggest that effects of wars on ecosystems may persist much longer than the wars themselves and that effects may have time-lags, particularly in cases where policies such as war reparations affect ecosystems for decades after the conflict ended (Fisunoglu, 2014; Kim et al., 2014; Organski and Kugler, 1977).

In order to quantify the environmental effects of WWII on Romania's forests, we developed an accurate and time-efficient method to orthorectify historical declassified satellite photography. Our new method is relevant to many disciplines concerned with land monitoring because Corona high-resolution data is available worldwide (Song et al., 2014), and our approach enables researchers and practitioners to extend the time-horizon of broad-scale analyses using satellite data from 1972, when the first Landsat was launched, to the early 1960s. The method is user-friendly, robust, time-efficient compared to photogrammetry methods (Galiatsatos et al., 2004; Sohn et al., 2004; Tappan et al., 2000), and it does not require ancillary information regarding camera position and conditions, (Beck et al., 2007; Casana and Cothren, 2008; Hamandawana et al., 2007; Ouédraogo et al., 2014; Peebles, 1997; Sohn et al., 2004; Zhou et al., 2003). Our method resulted in an average

Table 2
GCP error summaries.

	No. of points	Mean error(m)	Std. dev (m)	Median(m)	Min (m)	Max (m)	Range (m)
Total	941	14.3	8.8	13.5	0.3	43.4	43.1
Major relief units ($p < 0.001$)							
Mountains	436	20.2	8.2	20.9	0.3	43.4	43.1
Hills	424	10.3	5.3	10.0	0.5	21.7	21.3
Plains	81	3.58	1.2	3.7	1.0	6.0	4.9
Camera type ($p = 0.7805$)							
KH-4A	141	14.1	8.5	13.5	1.0	38.3	37.3
KH-4B	800	14.4	8.8	13.5	0.3	43.4	43.1
Image quality ($p < 0.001$)							
High	522	13.7	9.0	12.3	0.3	43.4	43.1
Medium	261	15.5	8.5	14.4	1.4	43.2	41.8
Low	158	14.7	8.3	14.0	1.2	36.0	34.8
Slope direction ($p = 0.6023$)							
North	3	9.8	8.1	8.7	2.3	18.4	16.2
North-East	40	14.1	7.9	13.5	2.9	43.4	40.5
East	135	13.9	9.0	13.3	1.7	39.1	37.4
South-East	224	14.3	8.8	13.4	1.0	38.3	37.2
South	231	14.4	8.6	13.2	0.7	43.2	42.6
South-West	166	13.9	8.6	13.4	0.3	35.4	35.1
West	111	15.1	8.9	14.4	1.0	37.7	36.7
North-West	31	15.8	9.9	12.3	1.5	38.4	36.9

horizontal positional error of only 14.3 m, comparable to previous studies that employed photogrammetric approaches for rectification of Corona, and the number of ground control points that were required for the rectification was only 20–30 points per image strip, compared with 35–250 points for photogrammetric approaches (Casana and Cothren, 2013, 2008; Fowler, 2004; Grosse et al., 2005; Hamandawana et al., 2007; Sohn et al., 2004; Zhou et al., 2003).

Corona photographs have high spatial resolution (up to 2 m), good spatial and temporal coverage, and are affordable. One image strip covers 3900 km^2 (Day, 2015; Sohn et al., 2004) and multiple images were typically recorded on the same day, making it possible to map large areas with high resolution data that is temporally consistent (Perry, 1973). The cost and the amount of data to be processed are lower when working with Corona (30$ per image strip) than when working with historic aerial photography. Furthermore, this approach can be easily applied to other aerial or satellite imagery with stereographic capabilities, and could therefore represent a valuable tool for historic land monitoring.

Our methodological advancement allowed us to quantify the time-lagged effect of WWII on Romania's forests. Countries of the former Eastern Bloc that were relatively undeveloped (Fisunoglu, 2014; Kim et al., 2014), such as Romania, likely experienced a delay in the Phoenix factor after WWII (Organski and Kugler, 1977). Our results show that effects of WWII lasted at least two decades, likely due to war reparation payments and related infrastructural development effects (Bereziuc, 2004; Ivanescu, 1972). Indeed, war reparations in form of natural resources are common in many parts of the world following conflict events (Parrini and Matray, 2002) and here we provide for the

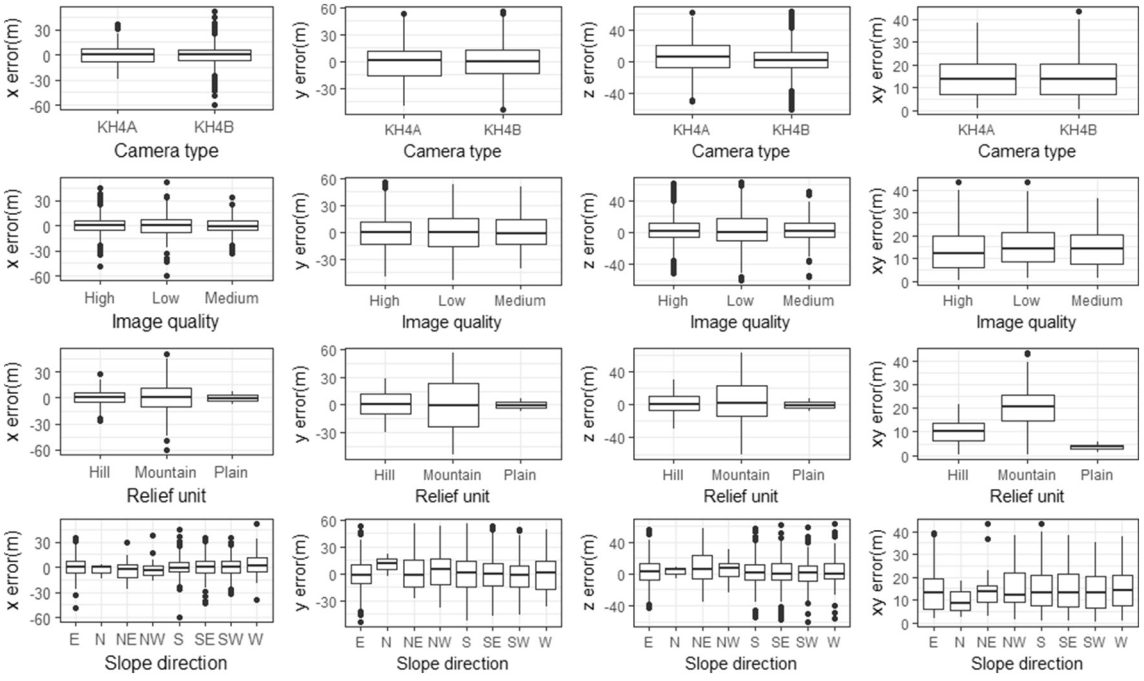

Fig. 5. Error distribution based on camera properties (Camera type and Image quality) and terrain (Relief unit and Slope direction).

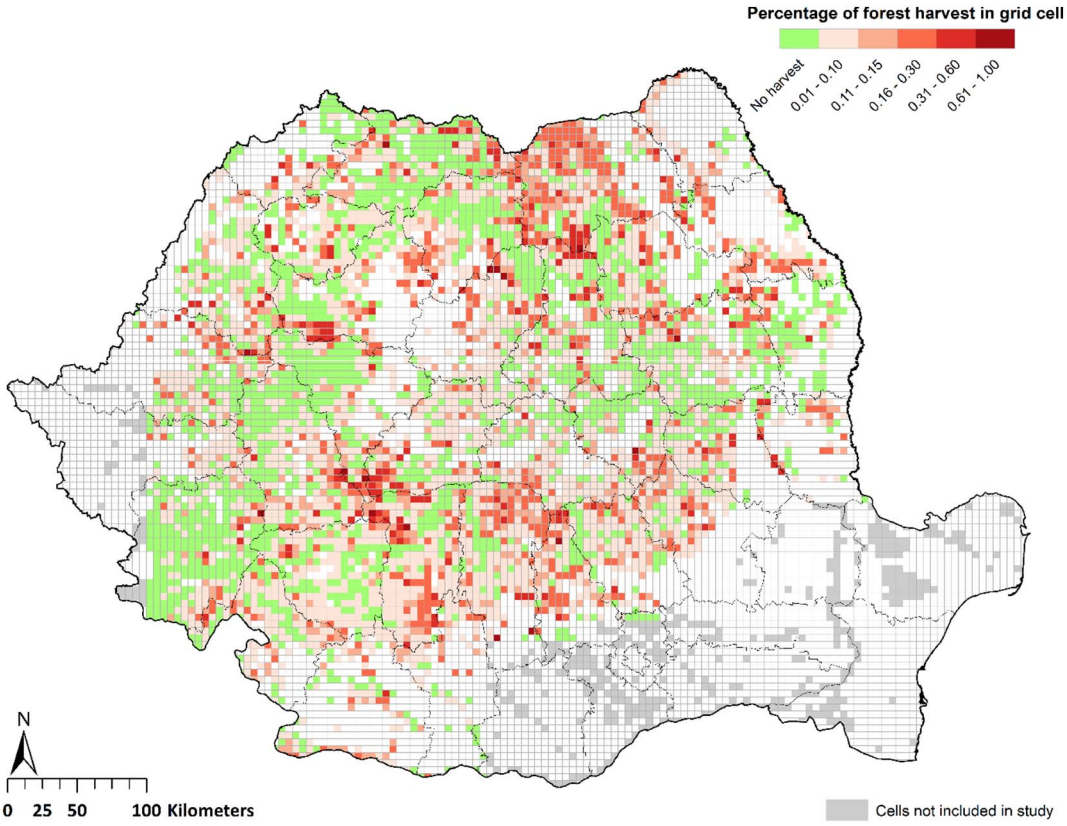

Fig. 6. Forest disturbances patterns summarized for 5-km grid cells (based on 1962–1966 photographs).

Table 3
Forest disturbance patch summaries.

	No of patches	Harvested area (ha)	Average patch size (ha)	Std. dev	Min patch size	Max patch size
Total	10,505	530,901.5	50.5	176.2	< 0.01	11,731.8
Major relief units						
Plains	598	13,071.0	21.9	31.5	< 0.01	373.8
Hills	5642	147,255.6	26.1	43.4	< 0.01	836.6
Mountains	4260	370,536.4	87.0	267.7	< 0.01	11,731.8
Main forest types						
Beech	3792	190,179.9	50.2	108.6	< 0.01	3186.2
Spruce	767	63,427.2	82.7	206.0	< 0.01	2770.8
Spruce-Beech Mix	1544	187,919.5	121.7	388.1	< 0.01	11,731.8
Others	1417	19,359.7	13.7	15.8	< 0.01	187.2
Oak	2985	70,015.3	23.5	33.2	< 0.01	481.6
Elevation (m)						
< 500	5704	148,278.6	26.0	43.0	< 0.01	836.6
500–1000	201	24,794.6	123.4	339.9	< 0.01	3186.2
1000–1500	1612	182,578.3	113.3	381.4	< 0.01	11,731.8
> 1500	2988	175,250.1	58.7	125.3	< 0.01	2125.6
Slope (degrees)						
< 5	1449	30,777.7	21.2	31.5	< 0.01	481.6
5–15	5261	200,203.8	38.1	99.6	< 0.01	3186.2
15–30	3668	296,137.9	80.7	269.7	< 0.01	11,731.8
> 30	127	3782.0	29.8	32.5	< 0.01	222.5

first time a solid estimate how this affected forest harvests.

In the context of Romanian forestry, our results highlighted the magnitude of forest harvesting after WWII partly due to war reparation agreement between Russia and Romania (Banu, 2004; Bekes et al., 2015; Ben-ner and Montias, 2015). This represents the first spatially explicit account of Cold War forest harvest for the region, and we mapped a total amount of 530,000 ha harvested forests. This value was twice as high as before WWII when the forest was harvested mainly for construction and fire wood. Prior reports suggested that Romania had agreed to pay war reparations to Russia by harvesting 256,000 ha of forest (Banu, 2004), and our results highlight that actual harvests were twice as much in order to cover both the reparations and regular demands. This trend continued even after Romania war reparations were paid in full in 1956. Furthermore, official reports from 1974 confirmed broad scale harvests between 1949 and 1964, when forest harvesting exceeded the sustainable thresholds by up to 47% countrywide (Marea Adunare Nationala, 1976). Most of those harvests were reported to have occurred in coniferous stands, which were harvested by as much as 104% above the sustainable level (Marea Adunare Nationala, 1976). Our results are consistent with reports that highlight major harvests in the regions of Neamt, Suceava and Bacau (Marea Adunare Nationala, 1976) but in addition to these regions, we found logging hotspots in Cluj, Hunedoara, Alba, Sibiu, Arges and Gorj.

We highlight that the majority of the harvests were clear cuts or final-cuts in shelterwood systems, and that mixed forest of spruce and beech were particularly affected by large-scale harvests, suggesting that the most valuable timber was especially targeted (Giurescu, 1976; Ivanescu, 1972). However, we caution that our analysis may have also captured wind throws or other natural disturbances, that we could not distinguish from harvests. Most of the disturbed forests were located in mountainous areas and in previously inaccessible valleys, which required new forest roads and narrow gage railways (Giurescu, 1976). This infrastructure development likely caused continued large-scale harvesting in areas that became newly accessible for forestry, even after the war reparation agreements between Russia and Romania ended (Giurgiu, 2010; Ivanescu, 1972). Our data capture these processes up to 1965 when a major political regime shift occurred in Romania, accompanied by changes in forest management (Tamas, 1987). In Romania, prior to the WWII, old forests (over 80 years) made up over 25%

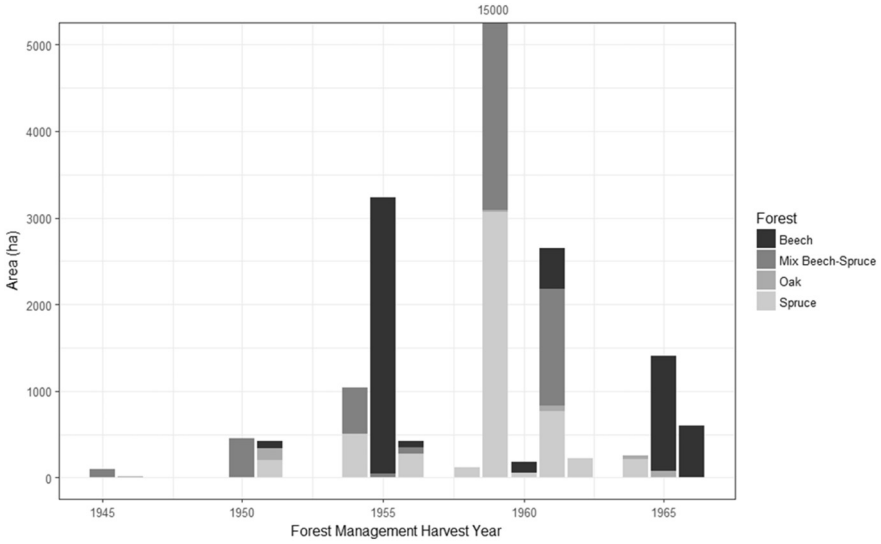

Fig. 7. Forest harvest year distribution based on forest management plans within the cross-checked disturbance polygons that we digitized based on Corona images. Forest types are indicated based on forest types following Corona mapped disturbance.

of all forests, but by 2010, this value had decreased to 21% (C. Munteanu et al., 2016). These reported decreases in old forests in Romania during the Socialist period may be related to the broad scale harvests that we show here. Furthermore, our analysis revealed one of the largest continuous disturbed areas (11,700 ha) ever identified in Romanian forestry.

More broadly, our findings make two major contributions to land-use science and remote sensing. We demonstrated the magnitude of time-lagged environmental effects of wars, which in Romania were also caused by war reparations and resulted in substantial changes in forest harvest and forest cover. This may also affect contemporary land management, land use change and conservation (Abrudan et al., 2009; Knorn et al., 2012). Historic land use and disturbance events can impact contemporary soils (Foster et al., 2003; Plue et al., 2008), vegetation patterns (Morris et al., 2011; Rhemtulla et al., 2009), and subsequent rates of forest change (Munteanu et al., 2017, 2015). In Romania, historic forest cover and historic deforestation affected both contemporary harvesting rates and forest composition (Munteanu et al., 2017, 2015). Although most of the historically harvested areas have returned to forest cover, the composition and structure of differs greatly, with potentially major implications for management and conservation (C. Munteanu et al., 2016). A back-of-the envelope calculation of contemporary forest composition of historically harvested patches (based on Corine Land Cover data 2012) shows that as much as 14% contemporary spruce cover was actually harvested during our researched time period, and likely replanted with monocultures, despite the fact that as much as 67% as the harvested areas were historically deciduous or mixed forests. Furthermore, of the historic harvests, 163.307 ha (32%) are currently spruce monocultures (also see Supplementary Figure No 1). Monocultures are prone to natural disturbances such as windthrows and bark beetle infestations. More broadly, we provide evidence for the broad-scale effects of political and economic shocks on natural resources at multiple temporal scales.

Overall, our methodological contribution to the field of remote sensing is that we developed a fast and efficient approach to extend satellite based land-use analyses into the past, based on Corona spy satellite photographs. Here, we used the case of Romanian forestry to show the time-lag effects of WWII on forest ecosystems in Romania, which may have long-term legacies up to today. We suggest that Corona photography, especially due to the stereoscopic capabilities (Galiatsatos et al., 2004) can be used for scientific inquiry in multiple fields such as geology, archeology, water and ice monitoring or vegetation monitoring. Our method unlocks the potential of such analysis at broad scales and for answering further remote sensing and ecological questions.

Acknowledgements

We thank three anonymous reviewers for their very insightful comments on an earlier version of this manuscript. We gratefully acknowledge support by the Romanian-US Fulbright Commission (Grant 601/2016), the National Aeronautics Space Administration (NASA) LCLUC Program, the NASA Earth System Science Fellowship Program (NESSF14/2014) and the Transilvania University of Brasov Fellowship Program for International Mobility (Grant 14.2/2016).

Appendix A. Supplementary data

Supplementary data to this article can be found online at https://doi.org/10.1016/j.rse.2017.10.021.

References

Abrudan, I.V., Marinescu, V., Ionescu, O., Ioras, F., Horodnic, S.A., Sestras, R., 2009. Developments in the Romanian forestry and its linkages with other sectors. Not. Bot. Hort. Agrobot. Cluj 37, 14–21.
Agisoft LLC, 2011. Agisoft PhotoScan User Manual.
Altmaier, A., Kany, C., 2002. Digital surface model generation from CORONA satellite images. ISPRS J. Photogramm. Remote Sens. 56, 221–235. http://dx.doi.org/10.1016/S0924-2716(02)00046-1.
ANCPI, 2010. Geoportal ANCPI [WWW Document]. (URL http://geoportal.ancpi.ro/geoportal/viewer/index.html (accessed 2.22.17)).
Apollonio, F.I., Ballabeni, A., Gaiani, M., Remondino, F., 2014. Evaluation of feature-based methods for automated network orientation. Int. Arch. Photogramm. Remote. Sens. Spat. Inf. Sci. 40, 47–54. http://dx.doi.org/10.5194/isprsarchives-XL-5-47-2014.
Bakacsi, G., Sándor, T., András, K., Viktor, I., 2002. Eastern European cluster: tradition and transition. J. World Bus. 37, 69–80. http://dx.doi.org/10.1016/S1090-9516(01)00075-X.
Bancila, A.M., 2016. Sovromurile, forma economica de sprijin reciproc, ascensiune şi decădere. Bull. the'Carol I'National Def. Univ. 3, 9–15.
Banu, F., 2004. Asalt asupra economiei Romaniei de la Solagra la SOVROM (1936–1956) (in Romanian). Nemira, Bucuresti.
Baumann, M., Kuemmerle, T., 2016. The impacts of warfare and armed conflict on land systems. J. Land Use Sci. 11, 672–688. http://dx.doi.org/10.1080/1747423X.2016.1241317.
Baumann, M., Radeloff, V.C., Avedian, V., Kuemmer, 2014. Land-use change in the Caucasus during and after the Nagorno-Karabakh conflict. Reg. Environ. Chang. http://dx.doi.org/10.1007/s10113-014-0728-3.
Beck, A., Philip, G., Abdulkarim, M., Donoghue, D., 2007. Evaluation of Corona and Ikonos high resolution satellite imagery for archaeological prospection in western Syria. Antiquity 81, 161–175. http://dx.doi.org/10.1017/S0003598X00094916.
Bekes, C., Borhi, L., Rugenthaler, P., Trasca, O., 2015. Soviet Occupation of Romania, Hungary and Austria 1944/45–1948/49, 1st ed. Central European University Press, Budapest.
Ben-ner, A., Montias, J.M., 2015. The introduction of markets in a hypercentralized economy: the case of Romania. J. Econ. Perspect. 5, 163–170.
Bereziuc, R., 2004. Realizari si perspective în domeniul cailor forestiere de transport. Analele Univ. “Stefan cel Mare”, Suceava, pp. 9–14.

Bindschadler, R., Vornberger, P., 1998. Changes in the West Antarctic ice sheet since 1963 from declassified satellite photography. Science ((80-.). 279).
Bouma, J., Varallyay, G., Batjes, N., 1998. Principal land use changes anticipated in Europe. Agric. Ecosyst. Environ. 67, 103–119. http://dx.doi.org/10.1016/S0167-8809(97)00109-6.
Brenner, R., 2003. The boom and the bubble: the US in the world economy. In: Verso.
Burgess, R., Miguel, E., Stanton, C., 2015. War and deforestation in Sierra Leone. Environ. Res. Lett. 10, 95014. http://dx.doi.org/10.1088/1748-9326/10/9/095014.
Burns, W.J., Coe, J.A., Kaya, B.S., Ma, L., 2010. Analysis of elevation changes detected from multi-temporal LiDAR surveys in forested landslide terrain in Western Oregon. Environ. Eng. Geosci. 16, 315–341. http://dx.doi.org/10.2113/gseegeosci.16.4.315.
Burns, J.H.R., Delparte, D., Gates, R.D., Takabayashi, M., 2015. Integrating structure-from-motion photogrammetry with geospatial software as a novel technique for quantifying 3D ecological characteristics of coral reefs. PeerJ 3, e1077. http://dx.doi.org/10.7717/peerj.1077.
Caroti, G., Martínez-Espejo Zaragoza, I., Piemonte, A., 2015. Accuracy assessment in Structure from Motion 3D reconstruction from UAV-born images: the influence of the data processing methods. Int. Arch. Photogramm. Remote. Sens. Spat. Inf. Sci. 40, 103–109. http://dx.doi.org/10.5194/isprsarchives-XL-1-W4-103-2015.
Casana, J., Cothren, J., 2008. Stereo analysis, DEM extraction and orthorectification of CORONA satellite imagery: archaeological applications from the Near East. Antiquity 82, 732–749. http://dx.doi.org/10.1017/S0003598X00097349.
Casana, J., Cothren, J., 2013. In: Comer, D.C., Harrower, M.J. (Eds.), The CORONA Atlas Project: Orthorectification of CORONA Satellite Imagery and Regional-Scale Archaeological Exploration in the Near East BT - Mapping Archaeological Landscapes from Space. Springer New York, New York, NY, pp. 33–43. http://dx.doi.org/10.1007/978-1-4614-6074-9_4.
Challis, K., Priestnall, G., Gardner, A., Henderson, J., O'Hara, S., 2002. Corona remotely-sensed imagery in dryland archaeology: the Islamic City of al-Raqqa, Syria. J. F. Archaeol. 29, 139. http://dx.doi.org/10.2307/3181489.
Clinciu, I., Nita, M.D., 2011. Using stereo matching 3D models in monitoring hydro-technical torrent control structures. Bull. Transilv. Univ. Braşov, Ser. II For. Wood Ind. Agric. Food Eng. 4, 7–12.
Constantinescu, M., 1953. Marele ajutor acordat de I.V. Stalin in dezvoltarea economiei tarilor de democratie populara. Scanteia 2.
Dashora, A., Lohani, B., Malik, J.N., 2007. A repository of earth resource information - CORONA satellite programme. Curr. Sci. 92, 926–932.
Day, D., 2015. Eye in the Sky: the Story of the CORONA Spy Satellites. Smithsonian Institution.
DeConde, A., 1978. A History of American Foreign Policy. Scribner.
Delparte, D.M., Belt, M., Nishioka, C., Turner, N., Richardson, R.T., Ericksen, T., 2014. Monitoring tropical alpine lake levels in a culturally sensitive environment utilizing 3D technological approaches. Arct. Antarct. Alp. Res. 46, 709–718. http://dx.doi.org/10.1657/1938-4246-46.4.709.
Dinca, L., Nita, M.D., Hofgaard, A., Alados, C.L., Broll, G., Borz, S.A., Wertz, B., Monteiro, A.T., 2017. Forests dynamics in the montane – alpine boundary: a comparative study using satellite imagery and climate data. Clim. Res. 73, 97–110. http://dx.doi.org/10.3354/cr01452.
Directia Topografica Militara, 1975. Harta Topografica scara 1:25000.
Doniţă, N., 2014. Etape în cartografi a pădurilor şi a învelişului vegetal din România 1. In: Bucovina For. 14, pp. 117–120.
Donita, N., Leandru, V., Puscaru-Soroceanu, E., 1960. Harta geobotanica R.P.R [Republica Populara Romana].
Eichengreen, B., 1945. Institutions and economic growth: Europe after World War II. In: Econ. Growth Eur. Since 38–72.
Fisunoglu, F.A., 2014. Beyond the Phoenix Factor: Consequences of Major Wars and Determinants of Postwar Recovery by. The Claremont Graduate University.
Foley, J. a, Defries, R., Asner, G.P., Barford, C., Bonan, G., Carpenter, S.R., Chapin, F.S., Coe, M.T., Daily, G.C., Gibbs, H.K., Helkowski, J.H., Holloway, T., Howard, E. a, Kucharik, C.J., Monfreda, C., Patz, J. a, Prentice, I.C., Ramankutty, N., Snyder, P.K., 2005. Global consequences of land use. Science 309, 570–574. http://dx.doi.org/10.1126/science.1111772.
Fonstad, M.A., Dietrich, J.T., Courville, B.C., Jensen, J.L., Carbonneau, P.E., 2013. Topographic Structure from Motion: a new development in photogrammetric measurement. Earth Surf. Process. Landf. 38. http://dx.doi.org/10.1002/esp.3366.
Foster, D.R., Swanson, F.J., Aber, J., Burke, I., Brokaw, N., Tilman, D., Knapp, A., 2003. The importance of land-use legacies to ecology and conservation. Bioscience 53, 77–88.
Fowler, M.J.F., 2004. Cover: declassified CORONA KH-4B satellite photography of remains from Rome's desert frontier. Int. J. Remote Sens. 25, 3549–3554. http://dx.doi.org/10.1080/0143116031000098887.
Fritts, T.H., Rodda, G.H., 1998. The role of introduced species in the degradation of island ecosystems: a case history of Guam. Annu. Rev. Ecol. Syst. 29, 113–140.
Galiatsatos, N., Donoghue, D.N.M., Philip, G., 2004. An Evaluation of the Stereoscopic Capabilities of CORONA Declassified Spy Satellite Image Data.
Geist, H.J., Lambin, E.F., 2004. Dynamic causal patterns of desertification. Bioscience 54, 817–829.
Gheyle, W., Bourgeois, J., Goossens, R., Jacobsen, K., 2011. Scan problems in digital CORONA satellite images from USGS archives Scan Problems in Digital CORONA Satellite Images from USGS Archives. Photogramm. Eng. Remote. Sens. 77, 1257–1264. http://dx.doi.org/10.14358/PERS.77.12.1257.
Gibianskii, L., Naimark, N.M., 2006. The soviet union and the establishment of communist regimes in Eastern Europe, 1944–1954. In: A Documentary Collection. Washington, D.C.
Giurescu, C., 1976. Istoria pădurii româneşti din cele mai vechi timpuri până astăzi.
Giurgiu, V., 2010. Consideraţii asupra stării pădurilor României - partea I: Declinul suprafeţei pădurilor şi marginalizarea împăduririlor. In: Rev. pădurilor.
Gomez, C., 2012. Historical 3D Topographic Reconstruction of the Iwaki Volcano Using Structure from Motion from Uncalibrated Aerial Photographs.
Grosse, G., Schirrmeister, L., Kunitsky, V.V., Hubberten, H.-W., 2005. The use of CORONA images in remote sensing of periglacial geomorphology: an illustration from the NE Siberian coast. Permafr. Periglac. Process. 16, 163–172. http://dx.doi.org/10.1002/ppp.509.
Hamandawana, H., Eckardt, F., Ringrose, S., 2007. Proposed methodology for georeferencing and mosaicking Corona photographs. Int. J. Remote Sens. 28, 5–22. http://dx.doi.org/10.1080/01431160500104400.
Hansen, M.C., Potapov, P.V., Moore, R., Hancher, M., Turubanova, S.A., Tyukavina, A., Thau, D., Stehman, S.V., Goetz, S.J., Loveland, T.R., Kommareddy, A., Egorov, A., Chini, L., Justice, C.O., Townshend, J.R.G., 2013. High-resolution global maps of 21st-century forest cover change. Science 342, 850–853. http://dx.doi.org/10.1126/science.1244693.
Harris, C., 1993. Geometry from visual motion. In: Active Vision. MIT press, pp. 263–284.
Harwin, S., Lucieer, A., 2012. Assessing the accuracy of georeferenced point clouds produced via multi-view stereopsis from Unmanned Aerial Vehicle (UAV) imagery. Remote Sens. 4, 1573–1599. http://dx.doi.org/10.3390/rs4061573.
Hasic, T., 2004. Reconstruction Planning in Post-conflict Zones: Bosnia and Herzegovina and the International Community. Royal Institute of Technology.
Heikkila, J., Silven, O., 1997. A four-step camera calibration procedure with implicit image correction. Proc. IEEE Comput. Soc. Conf. Comput. Vis. Pattern Recognit. 1106–1112. http://dx.doi.org/10.1109/CVPR.1997.609468.
Henley, S., 2012. Nonparametric Geostatistics. Springer Science & Business Media.
Herman, S., 1951. War damage and nationalization in Eastern Europe. Law Contemp. Probl. 16, 498. http://dx.doi.org/10.2307/1190167.
Humphreys, M., 2005. Natural resources, conflict, and conflict resolution. J. Confl. Resolut. 49, 508–537. http://dx.doi.org/10.1177/0022002705277545.
Ichino, A., Winter-Ebmer, R., 2004. The long-run educational cost of world war II. J. Labor Econ. 22, 57–87. http://dx.doi.org/10.1086/380403.
Isaev, A.S., Korovin, G.N., Bartalev, S.A., Ershov, D.V., Janetos, A., Kasischke, E.S., Shugart, H.H., French, N.H.F., Orlick, B.E., Murphy, T.L., 2002. Using remote sensing to assess Russian Forest fire carbon emissions. Clim. Chang. 55, 235–249. http://dx.doi.org/10.1023/A:1020221123884.
Ivanescu, D., 1972. Din istoria silviculturii romanesti. Ceres Publishing House, Bucharest.
Kadmon, R., Harari-Kremer, R., 1999. Studying long-term vegetation dynamics using digital processing of historical aerial photographs. Remote Sens. Environ. 68, 164–176. http://dx.doi.org/10.1016/S0034-4257(98)00109-6.
Kim, K.C., 1997. Preserving Biodiversity in Korea's Demilitarized Zone. Science ((80-.). 278).
Kim, K., Jezek, K., Liu, H., 2007. Orthorectified image mosaic of Antarctica from 1963 Argon satellite photography: image processing and glaciological applications. Int. J. Remote Sens. 28, 5357–5373. http://dx.doi.org/10.1080/01431160601105850.
Kim, T.-Y., Jeong, G., Lee, J., 2014. War, Peace and Economic Growth: The Phoenix Factor Reexamined. In: Economic Growth. Springer Berlin Heidelberg, Berlin, Heidelberg, pp. 263–278. http://dx.doi.org/10.1007/978-3-642-40826-7_8.
Knorn, J., Kuemmerle, T., Radeloff, V.C., Szabo, A., Mindrescu, M., Keeton, W.S., Abrudan, I., Griffiths, P., Gancz, V., Hostert, P., 2012. Forest restitution and protected area effectiveness in post-socialist Romania. Biol. Conserv. 146, 204–212. http://dx.doi.org/10.1016/j.biocon.2011.12.020.
Kozak, J., Estreguil, C., Vogt, P., 2007. Forest cover and pattern changes in the Carpathians over the last decades. Eur. J. For. Res. 126, 77–90.
Lambin, E.F., Geist, H.J., Lepers, E., 2003. Dynamics of land-use and land-cover change in tropical regions. Annu. Rev. Environ. Resour. 28, 205–241. http://dx.doi.org/10.1146/annurev.energy.28.050302.105459.
Lerma, J., Villaverde, V., García, A., Cardona, J., 2006. Close range photogrammetry and enhanced recording of Palaeolithic rock art. ISPRS Comm. V 146–154.
Lowe, D.G., 2004. Distinctive image features from. Int. J. Comput. Vis. 60, 91–110. http://dx.doi.org/10.1023/B:VISI.0000029664.99615.94.
Lucchese, L., 2005. Geometric calibration of digital cameras through multi-view rectification. Image Vis. Comput. 23, 517–539. http://dx.doi.org/10.1016/j.imavis.2005.01.001.
Machlis, G.E., Hanson, T., 2011. Warfare Ecology. Springer, Dordrecht, pp. 33–40. http://dx.doi.org/10.1007/978-94-007-1214-0_5.
Marea Adunare Nationala, 1976. Programul national pentru conservarea si dezvoltarea fondului forestier in perioada 1976–2010.
Martins, I., Costa, V., Porteiro, F.M., Santos, R.S., 2006. Temporal and spatial changes in mercury concentrations in the North Atlantic as indicated by museum specimens of glacier lanternfishBenthosema glaciale (Pisces: Myctophidae). Environ. Toxicol. 21, 528–532. http://dx.doi.org/10.1002/tox.20217.
McDonald, R.A., 1995. CORONA-success for space reconnaissance, a Look into the Cold-War, and a revolution for intelligence. Photogramm. Eng. Remote. Sens. 61, 689–720.
Morris, L.R., Monaco, T.a., Sheley, R.L., 2011. Land-use legacies and vegetation recovery 90 years after cultivation in Great Basin sagebrush ecosystems. Rangel. Ecol. Manag. 64, 488–497. http://dx.doi.org/10.2111/REM-D-10-00147.1.
Müller, D., Leitão, P.J., Sikor, T., 2013. Comparing the determinants of cropland abandonment in Albania and Romania using boosted regression trees. Agric. Syst. 117, 66–77. http://dx.doi.org/10.1016/j.agsy.2012.12.010.
Munteanu, C., Kuemmerle, T., Keuler, N.S., Müller, D., Balazs, P., Dobosz, M., Griffiths, P., Halada, L., Kaim, D., Király, G., Konkoly-Gyuró, É., Kozak, J., Lieskovský, J., Ostafin, K., Ostapowicz, K., Shandra, O., Radeloff, V.C., 2015. Legacies of 19th century land use shapes contemporary forest cover. Glob. Environ. Chang. 34, 83–94.
Munteanu, C., Nita, M.D., Abrudan, I.V., Radeloff, V.C., 2016. Historical forest management in Romania is imposing strong legacies on contemporary forests and their management. For. Ecol. Manag. 361, 179–193. http://dx.doi.org/10.1016/j.foreco.

2015.11.023.
Munteanu, C., Kuemmerle, T., Boltižiar, M., Lieskovský, J., Mojses, M., Kaim, D., Konkoly-Gyuró, É., Mackovčin, P., Müller, D., Ostapowicz, K., Radeloff, V.C., 2017. 19th century land-use legacies affect contemporary land abandonment in the Carpathians. Reg. Environ. Chang (in press).
National Reconnaissance Office, 2005. Review and Redaction Guide for Automatic Declassification of 25-Year-Old Information.
Organski, A.F.K., Kugler, J., 1977. The costs of major wars: the phoenix factor. Am. Polit. Sci. Rev. 71, 1347–1366. http://dx.doi.org/10.1017/S0003055400269657.
Ouédraogo, M.M., Degré, A., Debouche, C., Lisein, J., 2014. The evaluation of unmanned aerial system-based photogrammetry and terrestrial laser scanning to generate DEMs of agricultural watersheds. Geomorphology 214, 339–355. http://dx.doi.org/10.1016/j.geomorph.2014.02.016.
Parrini, C., Matray, J., 2002. Reparations. Encycl. Am. Foreign Policy.
Peebles, C., 1997. The Corona Project. In: America's First Spy Sattelites. Naval Institute Press, Annapolis, Maryland.
Perry, R., 1973. A History of Satellite Reconaissance.
Plue, J., Hermy, M., Verheyen, K., Thuillier, P., Saguez, R., Decocq, G., 2008. Persistent changes in forest vegetation and seed bank 1,600 years after human occupation. Landsc. Ecol. 23, 673–688. http://dx.doi.org/10.1007/s10980-008-9229-4.
Pollefeys, M., Koch, R., Van Gool, L., 1999. Self-calibration and metric reconstruction inspite of varying and unknown intrinsic camera parameters. Int. J. Comput. Vis. 32. http://dx.doi.org/10.1023/A:1008109111715.
Popescu, S.C., Wynne, R.H., Nelson, R.F., 2003. Measuring individual tree crown diameter with lidar and assessing its influence on estimating forest volume and biomass. Can. J. Remote. Sens. 29, 564–577. http://dx.doi.org/10.5589/m03-027.
Potapov, P.V., Turubanova, S.a., Tyukavina, A., Krylov, A.M., McCarty, J.L., Radeloff, V.C., Hansen, M.C., 2015. Eastern Europe's forest cover dynamics from 1985 to 2012 quantified from the full Landsat archive. Remote Sens. Environ. 159, 28–43. http://dx.doi.org/10.1016/j.rse.2014.11.027.
Rhemtulla, J.M., Mladenoff, D.J., Clayton, M.K., 2009. Legacies of historical land use on regional forest composition and structure in Wisconsin, USA (mid-1800s-1930s-2000s). Ecol. Appl. 19, 1061–1078.
Rigina, O., 2003. Detection of boreal forest decline with high-resolution panchromatic satellite imagery. Int. J. Remote Sens. 24, 1895–1912. http://dx.doi.org/10.1080/01431160210154894.
Robinson, R.A., Sutherland, W.J., 2002. Post-war changes in arable farming and biodiversity in Great Britain. J. Appl. Ecol. 39, 157–176. http://dx.doi.org/10.1046/j.1365-2664.2002.00695.x.
Roy, D.P., Wulder, M.A., Loveland, T.R., W., C.E., Allen, R.G., Anderson, M.C., Helder, D., Irons, J.R., Johnson, D.M., Kennedy, R., Scambos, T.A., Schaaf, C.B., Schott, J.R., Sheng, Y., Vermote, E.F., Belward, A.S., Bindschadler, R., Cohen, W.B., Gao, F., Hipple, J.D., Hostert, P., Huntington, J., Justice, C.O., Kilic, A., Kovalskyy, V., Lee, Z.P., Lymburner, L., Masek, J.G., McCorkel, J., Shuai, Y., Trezza, R., Vogelmann, J., Wynne, R.H., Zhu, Z., 2014. Landsat-8: science and product vision for terrestrial global change research. Remote Sens. Environ. 145, 154–172. http://dx.doi.org/10.1016/j.rse.2014.02.001.
Rudel, T.K., Coomes, O.T., Moran, E., Achard, F., Angelsen, A., Xu, J., Lambin, E., 2005. Forest transitions: towards a global understanding of land use change. Glob. Environ. Chang. 15, 23–31. http://dx.doi.org/10.1016/j.gloenvcha.2004.11.001.
Slama, C.C., Theurer, C., Henriksen, S.W., 1980. Manual of Photogrammetry. American Society of photogrammetry.
Sohn, H.-G., Kim, G.-H., Yom, J.-H., 2004. Mathematical modelling of historical reconnaissance CORONA KH-4B imagery. Photogramm. Rec. 19, 51–66. http://dx.doi.org/10.1046/j.0031-868X.2003.00257.x.
Song, D.X., Huang, C., Sexton, J.O., Channan, S., Feng, M., Townshend, J.R., 2014. Use of landsat and corona data for mapping forest cover change from the mid-1960s to 2000s: case studies from the Eastern United States and Central Brazil. ISPRS J. Photogramm. Remote Sens. 103, 81–92. http://dx.doi.org/10.1016/j.isprsjprs.2014.09.005.
Spârchez, G., Târziu, D.R., Dincă, L., 2013. Pedologie cu elemente de geologie și geomorfologie. Ed. Univ. Transilv. din Brașov.
geo-spatial.org, 2008. Harta unităților de relief din România [WWW Document]. (URL http://www.geo-spatial.org/download/harta-unitati-relief-romania (accessed 2.23.17)).
Tamas, R., 1987. Soviet economic impact on Czechoslovakia and Romania in the early postwar period: 1944–1956. In: Occasional Paper/East European Program. European Institute.
Tappan, G.G., Hadj, A., Wood, E.C., Lietzow, R.W., 2000. Use of Argon, Corona, and Landsat Imagery to Assess 30 Years of Land Resource Changes in West-Central Senegal. Vol. 66. pp. 727–735.
Ullman, S., 1979. The interpretation of Structure from Motion. Proc. R. Soc. Lond. Ser. B Biol. Sci. 203 (405) (LP-426).
USGS, 2004. Shuttle radar topography mission [WWW Document]. In: Glob. L. Cover Facil. Univ. Maryl, (URL http://www.landcover.org/data/srtm/).
Verhoeven, G., Doneus, M., Briese, C., Vermeulen, F., 2012. Mapping by matching: a computer vision-based approach to fast and accurate georeferencing of archaeological aerial photographs. J. Archaeol. Sci. 39, 2060–2070. http://dx.doi.org/10.1016/j.jas.2012.02.022.
Vorovencii, I., 2014. A change vector analysis technique for monitoring land cover changes in Copsa Mica, Romania, in the period 1985–2011. Environ. Monit. Assess. 186, 5951–5968. http://dx.doi.org/10.1007/s10661-014-3831-5.
Watson, G.A., 2006. Computing Helmert transformations. J. Comput. Appl. Math. 197, 387–394. http://dx.doi.org/10.1016/j.cam.2005.06.047.
Zhou, G., Jezek, K., Allen, T.R., 2003. Greenland Ice Sheet Mapping Using 1960s DISP Imagery 0. pp. 7929–7931.